Layer-by-layer three-dimensional chiral photonic crystals

M. Thiel,[1,*] G. von Freymann,[1,2] and M. Wegener[1,2]

[1]*Institut für Angewandte Physik and DFG-Center for Functional Nanostructures (CFN), Universität Karlsruhe (TH), Wolfgang-Gaede-Straße 1, D-76131 Karlsruhe, Germany*

[2]*Institut für Nanotechnologie, Forschungszentrum Karlsruhe in der Helmholtz-Gemeinschaft, Postfach 3640, D-76021 Karlsruhe, Germany*

[*]*Corresponding author: michael.thiel@physik.uni-karlsruhe.de*

Received June 13, 2007; accepted July 14, 2007;
posted July 31, 2007 (Doc. ID 84110); published August 20, 2007

We fabricate and characterize polymeric three-dimensional layer-by-layer chiral photonic crystals. The obtained circular dichroism from polarization stop bands is comparable with that of recently demonstrated circular–spiral photonic crystals. Moreover, telecommunication wavelengths are easily accessible with the layer-by-layer approach; even visible wavelengths are in reach. © 2007 Optical Society of America

OCIS codes: 160.4670, 260.5430.

Periodic chiral dielectric [1–3] or metallic [4–8] nanostructures have recently attracted considerable attention because of the possibility of obtaining giant circular dichroism [1–3,7] or giant gyrotropy [5,6,8] in the optical regime. At present, chiral dielectric structures outperform chiral metallic structures by a large margin regarding losses. Interesting dielectric candidates are the recently introduced circular–spiral designs [1,3], three-dimensional nanostructures of considerable complexity. While it is conceivable that high-quality circular–spiral structures might be fabricated on large areas at low cost via holographic lithography [9], it would be highly desirable to have blueprints at hand that are accessible by a variety of different approaches suitable for large-area low-cost mass fabrication. Regarding a distinct class of periodic structures, namely, photonic-bandgap materials, layer-by-layer approaches such as the famous woodpile structure [10] have proven to be accessible by a large variety of different techniques. Thus, chiral layer-by-layer structures appear to be attractive as well.

A recent theoretical paper [11] has indeed discussed chiral dielectric layer-by-layer structures. It is the aim of this Letter to provide corresponding experiments for what we believe to be the first time and to highlight that excellent performance can even be obtained with low refractive index contrast from polymeric structures.

The underlying idea [11] is quite simple and resembles models for cholesteric liquid crystals [12]: a first layer (in air) consists of a periodic arrangement of parallel dielectric rods or bars with refractive index n separated by the spacing a. A second identical layer is rotated by an angle of $360°/N$ and placed on top of the first layer. After an integer N number of layers, the structure obviously repeats itself, leading to the lattice constant c. In a loose sense, the resulting three-dimensional photonic crystal can be viewed as a "twisted woodpile." It should be immediately clear that the integers $N=1$, 2, and 4 do not lead to chiral structures, whereas the choices $N=3$, 5, 6, 7, etc. do. Depending on whether the stacking process is performed clockwise or counterclockwise with respect to the substrate, one can either obtain left-handed or right-handed chiral structures.

Such chiral structures can lead to polarization stop bands: in this spectral range and for one propagation direction, transmission of light is suppressed for one of the two circular polarizations. We have previously introduced the intuitive reasoning that a chiral resonance occurs if the pitch of the dielectric chiral structure matches the pitch of the circularly polarized light, i.e., if the lattice constant c matches the material wavelength of light [3]. This means that, for a

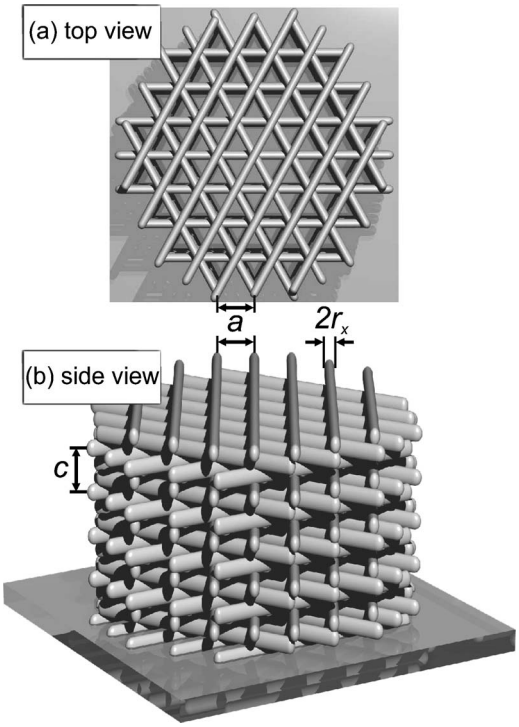

Fig. 1. Scheme of the chiral layer-by-layer photonic crystal structure for $N=3$. (a) Top view, (b) side view. The geometrical parameters are: $a=1.2$ μm, $c=1.32$ μm, $2r_x=300$ nm, and 15 layers (five lattice constants).

0146-9592/07/172547-3/$15.00

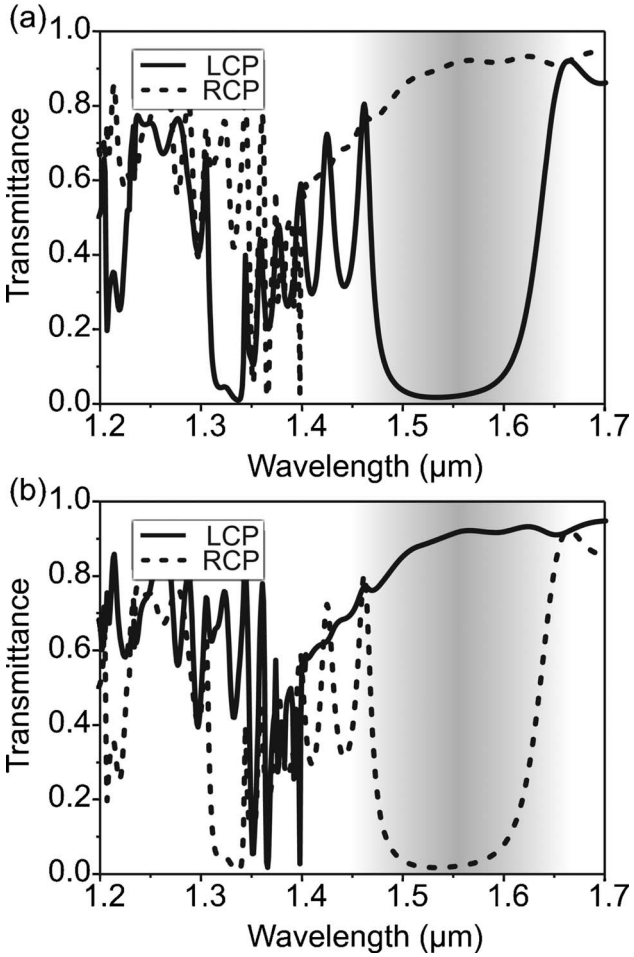

Fig. 2. Calculated normal-incidence linear-optical transmittance spectra for circular incident polarization. (a) Left-handed structure with the parameters given in Fig. 1 but with 24 layers (i.e., eight lattice constants); (b) right-handed structure for LCP incident light (solid) and RCP incident light (dashed).

fixed operation wavelength, the fabrication requires finer features with increasing N. Thus, small values of N are highly desirable. Furthermore, it is important to know what refractive index n is necessary for good performance. Reference [11] discussed a high-index-contrast material with refractive index $n=2.98$.

Our numerical calculations show that comparable performance can be achieved with low refractive indices. For the calculation of transmittance spectra of finite-size structures we employ the established scattering-matrix approach [13,14] and choose $n=1.57$ and $N=3$. We then search for optimum performance regarding circular dichroism by varying the c/a ratio and the volume filling fraction, f, of the dielectric. We find that rods with circular cross section (rather than elliptical) are best. The choice shown in Fig. 1 corresponds to the smallest ellipticity (approximately a 1.7 aspect ratio) that we are presently able to achieve experimentally by means of direct-laser writing [15,16] (see below) and to the parameters $c/a=1.1$ and $f=23.1\%$.

Figure 2 reveals calculated transmittance spectra for circularly polarized incident light impinging under normal incidence for the parameters of Fig. 1 and for 24 layers (i.e., eight lattice constants). Pronounced polarization stop bands, centered at an ~ 1.55 μm wavelength, are clearly visible: the transmittance is $\sim 91\%$ for right-handed circular incident polarization (RCP) impinging on a left-handed structure [Fig. 2(a)] and $\sim 2\%$ for left-handed circular incident polarization (LCP) and the same structure. As expected for ideal structures without unintentional linear birefringence, LCP and RCP interchange for a right-handed structure [Fig. 2(b)].

Notably, the overall performance is comparable with that of circular–spiral structures that we have previously presented [3] and that are much harder to fabricate. Also, the present twisted woodpile is mechanically much more robust than the laterally disconnected circular–spiral arrays. Moreover, for a given resolution of the direct-laser-writing process, shorter-wavelength polarization stop bands can be achieved in twisted woodpiles as compared with circular–spiral structures.

Next, we fabricate this optimized structure (Fig. 1) by means of standard direct-laser writing in the commercially available photoresist SU-8 (for details see, e.g., [16]). We emphasize, however, that this demonstration should be interpreted only as a proof of principle. Much larger-area structures could be fabricated by repeated microcontact printing, by hot embossing, or by other inexpensive mass-fabrication approaches. Electron micrographs are depicted in Fig. 3. The high quality and homogeneity of the structures are obvious. The structures are stabilized

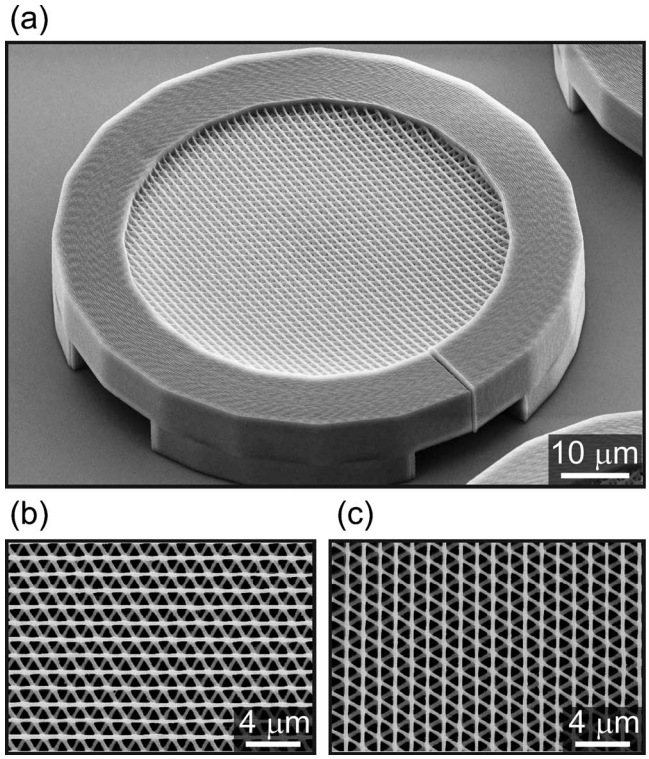

Fig. 3. Electron micrographs of fabricated structures with the parameters given in Fig. 1 but with 24 layers. (a) Oblique view of a complete structure with an open aperture of 60 μm diameter. (b) and (c) are top-view magnifications of left-handed and right-handed structures, respectively.

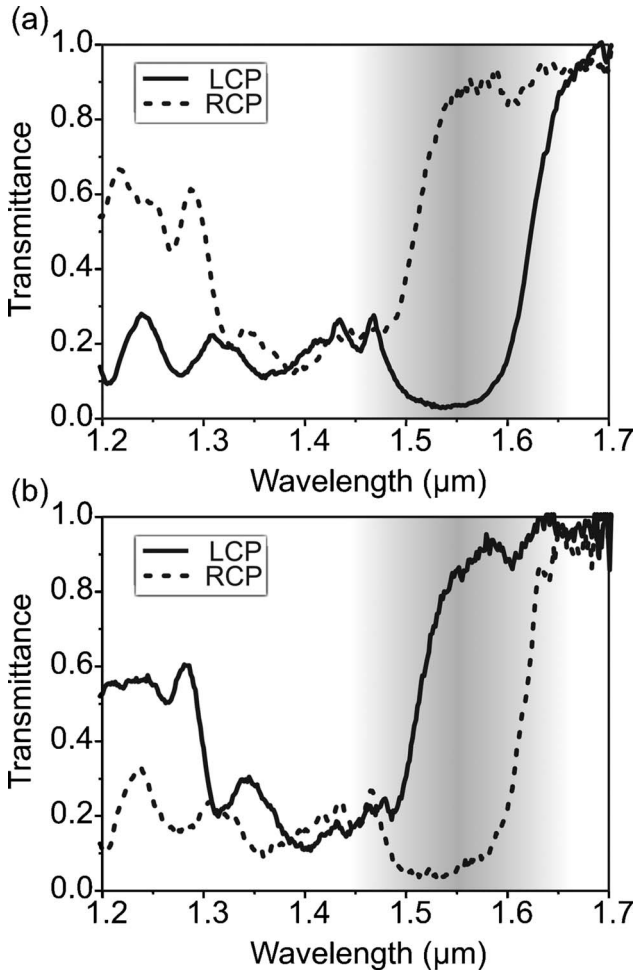

Fig. 4. Measured normal-incidence transmittance spectra for circular incident polarization, represented as the corresponding calculated spectra shown in Fig. 2.

by a surrounding thick wall [16], which is intentionally written higher than the top of the photonic crystal.

Corresponding optical characterization [3] is shown in Fig. 4, which is represented as Fig. 2 to allow for a direct comparison with the theory of a perfect structure. The incident circular polarization is accomplished by a Glan–Thompson polarizer followed by a superachromatic quarter-wave plate [3]. Obviously, the overall qualitative agreement between theory (Fig. 2) and experiment (Fig. 4) is very good. Specifically, the agreement in the region of the polarization stop band (gray area) is almost quantitative. On the short-wavelength side (i.e., for the higher-order bands), deviations arise, which are likely due to two aspects. First, the incident light in the experiment has a finite opening angle (5°), whereas the calculations are for strictly normal incidence. We have previously discussed [3] that this aspect affects the spectral shape. Second, the imperfections of the fabricated samples are expected to influence the higher-order bands more strongly.

In conclusion, we have presented low-index-contrast three-dimensional layer-by-layer chiral photonic crystals that show giant circular dichroism at telecommunication wavelengths. In the polarization stop band, this “thin-film” structure converts unpolarized incident light into circularly polarized emerging light. Moreover, circularly polarized incident light with the opposite handedness than the chiral structure is fully transmitted. After backreflection from a mirror behind the photonic crystal, the handedness of light is changed. Hence, the backward propagating light is not transmitted by the photonic crystal and does not propagate back into the light source. In this sense, the structure can serve as a “poor-man’s” optical isolator for circular polarization [17].

We acknowledge support by the Deutsche Forschungsgemeinschaft (DFG) and the State of Baden-Württemberg through the DFG-Center for Functional Nanostructures (CFN) within subproject A1.4. The research of G. von Freymann is further supported through a DFG Emmy Noether fellowship (DFG-Fr 1671/4-3). The Ph.D. education of M. Thiel is further supported by the Karlsruhe School of Optics and Photonics (KSOP).

References

1. J. Lee and C. T. Chan, Opt. Express **13**, 8083 (2005).
2. P. C. P. Hrudey, B. Szeto, and M. J. Brett, Appl. Phys. Lett. **88**, 251106 (2006).
3. M. Thiel, M. Decker, M. Deubel, M. Wegener, S. Linden, and G. von Freymann, Adv. Mater. **19**, 207 (2007).
4. A. Papakostas, A. Potts, D. M. Bagnall, S. L. Prosvirnin, H. J. Coles, and N. I. Zheludev, Phys. Rev. Lett. **90**, 107404 (2003).
5. M. Kuwata-Gonokami, N. Saito, Y. Ino, M. Kauranen, K. Jefimovs, T. Vallius, J. Turunen, and Y. Svirko, Phys. Rev. Lett. **95**, 227401 (2005).
6. A. V. Rogacheva, V. A. Fedotov, A. S. Schwanecke, and N. I. Zheludev, Phys. Rev. Lett. **97**, 177401 (2006).
7. M. Decker, M. W. Klein, M. Wegener, and S. Linden, Opt. Lett. **32**, 856 (2007).
8. E. Plum, V. A. Fedotov, A. S. Schwanecke, N. I. Zheludev, and Y. Chen, Appl. Phys. Lett. **90**, 223113 (2007).
9. Y. K. Pang, J. C. W. Lee, H. F. Lee, W. Y. Tam, C. T. Chan, and P. Sheng, Opt. Express **13**, 7615 (2005).
10. K.-M. Ho, C. T. Chan, C. M. Soukoulis, R. Biswas, and M. Sigalas, Solid State Commun. **89**, 413 (1994).
11. J. C. W. Lee and C. T. Chan, Appl. Phys. Lett. **90**, 051912 (2007).
12. H. de Vries, Acta Crystallogr. **4**, 219 (1951).
13. D. M. Whittaker and I. S. Culshaw, Phys. Rev. B **60**, 2610 (1999).
14. S. G. Tikhodeev, A. L. Yablonskii, E. A. Muljarov, N. A. Gippius, and T. Ishihara, Phys. Rev. B **66**, 045102 (2002).
15. S. Kawata, H.-B. Sun, T. Tanaka, and K. Takada, Nature **412**, 697 (2001).
16. M. Deubel, G. von Freymann, M. Wegener, S. Pereira, K. Busch, and C. M. Soukoulis, Nat. Mater. **3**, 444 (2004).
17. G. Shvets, Appl. Phys. Lett. **89**, 141127 (2006).